

## Staggering in low-spin nuclear spectra of $\gamma$ -soft or triaxial nuclei

Liao Ji-zhi

*China Center of Advanced Science and Technology (World Laboratory), P.O. Box 8730, Beijing 100080, People's Republic of China*  
*and Department of Physics, Sichuan Union University, Chengdu 61064, Sichuan, People's Republic of China*  
 (Received 8 June 1994)

The  $\gamma$ - or quasi- $\gamma$ -band energy staggering in low-spin, low-energy spectra of even-even nuclei is discussed. The staggering indices of  $\gamma$ -soft and triaxial nuclei are calculated in the interacting boson model O(6) limit with three-body potential and general axially asymmetric rotor model with  $\beta$  vibration, respectively. It is found that these staggering indices have opposite signs and provide clear distinctions between  $\gamma$ -soft and triaxial shapes. The experimental data of energy spectra of 140 of even-even nuclei in the mass region  $A = 64$  to 200 are compared to the predictions for broken O(6) symmetry with varying strength of the three-body interaction, and for the axially asymmetric rotor model with varying  $\gamma$  dependence. The results show that most nuclei with clear staggering are  $\gamma$  soft or  $\gamma$  unstable, but a few may be slightly triaxial, and that almost all the axial nuclei are slightly  $\gamma$  soft, some of them exhibiting shape transitions from axial to  $\gamma$ -soft to triaxial shape with increasing angular momentum.

PACS number(s): 21.10.Re, 21.60.Fw, 21.60.Ev

### I. INTRODUCTION

It is well known that the signature splitting effect in the rotational band is an important structural indicator in the study of rotational alignment in high-spin states [1]. The same effect is referred to as energy staggering in the  $\gamma$  or quasi- $\gamma$  band in low-spin, low-energy states of O(6)-like nuclei [2], or O(5)  $\gamma$ -soft nuclei [3]. The energy staggering is also present in the spectra of triaxial nuclei but with an alternative sequence. Recently, the question of whether axially asymmetric atomic nuclei are  $\gamma$  soft or  $\gamma$  rigid (triaxial) has been discussed by Zamfir and Casten [4]. They work in the interacting boson model (IBM) O(6) limit with a cubic term [5] for  $\gamma$ -soft nuclei and in the Davydov model [6] for triaxial nuclei. They use staggering indices  $S(J, J - 1, J - 2)$  defined as

$$S(J, J - 1, J - 2) = [(E_J - E_{J-1}) - (E_{J-1} - E_{J-2})]/E_{2g} \quad (1a)$$

as useful signatures that clearly distinguish  $\gamma$ -soft and  $\gamma$ -rigid potentials. They have examined the values of the staggering indices  $S(4,3,2)$  and  $S(6,5,4)$  obtained from the empirical levels of even-even nuclei with  $Z \geq 30$ , and concluded that nuclei with substantial asymmetry were found to be  $\gamma$  soft in the low-energy region, showing no evidence of  $\gamma$  rigidity [4].

It is the purpose of this work to indicate whether the above conclusion will be changed when we take into account the experimental level data up to spin  $I = 12$  and work in a more general broken O(6) symmetry of IBM1 with three-body potential [7] for  $\gamma$ -soft nuclei and in a general asymmetric rotor model with rotation-vibration interaction [8] for  $\gamma$ -rigid nuclei. In this work we adopt the following staggering index, which has opposite sign to that used by Casten *et al.* [9]:

$$S(I) = 1 - R(E_I)/R(E_I)_{\text{rotor}}, \quad (1b)$$

$$R(E_I) = 2(E_I - E_{I-1})/(E_I - E_{I-2}), \quad (1c)$$

where  $R(E_I)_{\text{rotor}}$  is  $R(E_I)$  for a rigid axial rotor, given by  $I/(I - \frac{1}{2})$ . Evidently, for an ideal axial rigid rotor  $S(I) = 0$  for all  $I$ .  $S(I)$  have positive or negative values depending on the pattern of the energy staggering as shown in Fig. 1. If a  $\gamma$  band contains levels arranged in almost degenerate couplets as  $2^+, (3^+, 4^+), (5^+, 6^+), (7^+, 8^+), \dots$ , then all the  $S(I_{\text{even}}) > 0$  and  $S(I_{\text{odd}}) < 0$ . This staggering pattern is a prediction for the  $\gamma$  band in the  $\gamma$ -unstable O(6) limit or in O(5) symmetry of the IBM. In contrast, if the staggering has the pattern  $2^+, 3^+, (4^+, 5^+), (6^+, 7^+), (8^+, 9^+), \dots$ , then all the  $S(I_{\text{even}}) < 0$  and  $S(I_{\text{odd}}) > 0$ . This is just the case for the  $\gamma$  band of a triaxial rotor. In both cases  $S(I)$  are

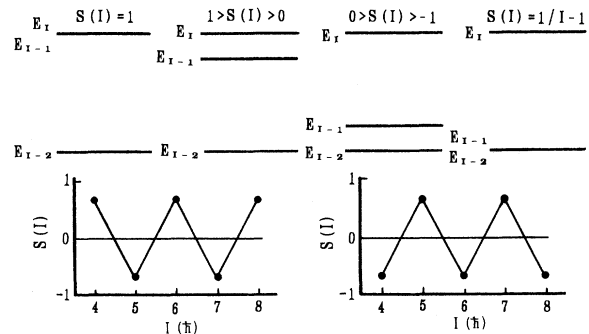


FIG. 1. Behavior of staggering indices  $S(I)$  for two kinds of energy spectra with significant staggering, showing exactly opposite zigzag phases.

oscillating with spin  $I$ , but with exactly opposite peaks and valleys (zigzag behavior) as shown in the lower part of Fig. 1. For convenience we say that  $S(I)$  has positive zigzag phase if all  $S(I_{\text{even}}) > 0$ , or has negative zigzag phase if all  $S(I_{\text{even}}) < 0$ .

## II. MODEL DESCRIPTION OF ENERGY STAGGERING

As mentioned above the energy staggering of  $\gamma$ -soft and  $\gamma$ -rigid nuclei is different. First, we study  $\gamma$ -soft nuclei in our broken  $O(6)$  symmetry of the IBM1 with three-body potential [briefly described as broken  $O(6)$  symmetry in the following] [7]. The Hamiltonian reads

$$H = AC_{2O(6)} + B'C_{2O(5)} + C'C_{2O(3)} + V_3, \quad (2a)$$

$$V_3 = P(n_d - 2)[(d^\dagger \tilde{d})^{(2)} \cdot (d^\dagger \tilde{d})^{(2)} - n_d], \quad (2b)$$

where  $C_{2O(6)}$ ,  $C_{2O(5)}$ , and  $C_{2O(3)}$  are the quadratic Casimir operators for  $O(6)$ ,  $O(5)$ , and  $O(3)$  groups, respectively,  $V_3$  is the three-body potential, and  $P$  its strength parameter. The Hamiltonian in Eq. (2) can be diagonalized in  $O(6)$  eigenfunctions  $[[N], \sigma, \tau, \nu, LM)$ . Then we obtain an approximate formula for the energy spectra with three parameters [7],

$$E_I = B\tau(\tau + 3) + CI(I + 1) - P[16\tau^2(\tau + 3)^2 + I^2(I + 1)^2]/N^2, \quad (3)$$

where  $\tau$  is the quantum number of group  $O(5)$ ,  $I$  the angular momentum, and  $N$  the boson number;  $B$ ,  $C$ , and  $P$  are free parameters, whose values can be determined by fitting the experimental energy spectra. In order to study the general behavior of the energy staggering in the spectra from Eq. (3), we consider an example. Let  $B = 62$  keV,  $C = 12$  keV, and  $N = 8$ ; the energy spectra up to  $I = 12$  of the ground state band and the  $\gamma$  band can be calculated for different values of parameter  $P$  between 0 and 12 keV. Then with the spectra of the  $\gamma$  band we get  $S(I)$  as functions of the strength parameter  $P$ . The calculated  $S(I_{\text{even}})$  for  $I = 4-12$  are given in Fig. 2.

Now for triaxial nuclei we consider the general axially asymmetric rotor model with rotation-vibration interaction [8,10] (briefly described as the asymmetric ro-

tor model in the following). It is assumed in this model that the rotational constants  $A$ ,  $B$ , and  $C$ , which depend on the moments of inertia  $J_A$ ,  $J_B$ , and  $J_C$ , are ordered according to [10]

$$A = \hbar/4\pi J_A \geq B = \hbar/4\pi J_B \geq C = \hbar/4\pi J_C,$$

and the energy  $E_b$  of the  $n$  level with angular momentum  $I$  is given in units of  $\hbar C$  by

$$E_b(k, I_n, A/C) = \varepsilon_0 - b\varepsilon_0^2, \quad (4a)$$

where

$$\varepsilon_0(k, I_n, A/C)$$

$$= I(I + 1)\{\beta(k, I_n) + (A/C)[1 - \beta(k, I_n)]\}, \quad (4b)$$

$$k = (2B - A - C)/(A - C). \quad (4c)$$

The functions  $\beta(k, I_n)$  are tabulated in Ref. [11]. It can be shown that for the levels  $2^+$  Eq. (4b) gives the same energies as those given by

$$E_2 = 9\hbar^2[1 \pm \sqrt{1 - 8 \sin^2 3\gamma/9}]/(J_0 \sin^2 3\gamma). \quad (4d)$$

When we precisely solve the eigenvalue problem of the asymmetric rotor we obtain

$$E_2 = \frac{9\hbar^2[1 \pm \sqrt{1 - 8(\sin^2 3\gamma + 4 \sin^6 \gamma - 4 \sin^8 \gamma)/9}]}{(J_0 \sin^2 3\gamma)}. \quad (5)$$

For very small asymmetric angle  $\gamma$  terms containing  $\sin^6 \gamma$  and  $\sin^8 \gamma$  may be omitted so that Eqs. (5) and (4d) give the same values. But for  $\gamma = 30^\circ$  there is an energy deviation amounting to  $\sim 10\%$  between Eq. (4d) and Eq. (5). In order to obtain more precise solutions of the asymmetric rotor we adopt the following diagonalization method. The Hamiltonian of the axially asymmetric rotor reads

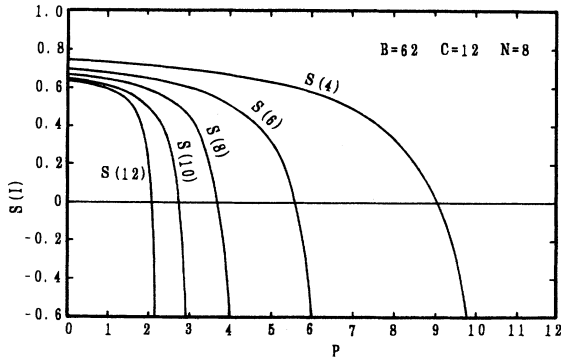


FIG. 2. Staggering indices  $S(I_{\text{even}})$  of a  $\gamma$ -soft rotor as functions of the strength parameter  $P$  for a three-body interaction.

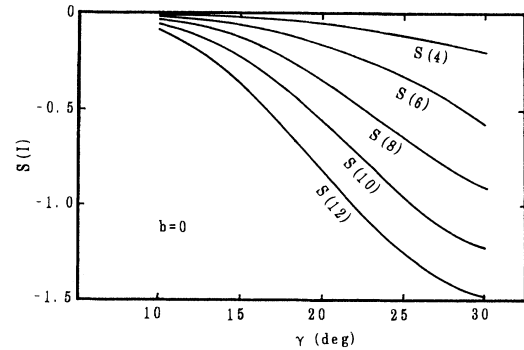


FIG. 3. Staggering indices  $S(I_{\text{even}})$  of a  $\gamma$ -rigid rotor for  $I = 4-12$  as functions of the asymmetric angle  $\gamma$ .

$$H = \left( \frac{\hbar^2}{4J_1} + \frac{\hbar^2}{4J_2} \right) (\hat{L}^2 - \hat{L}_3^2) + \frac{\hbar^2}{2J_3} \hat{L}_3^2 + \frac{\hbar^2}{8} \left( \frac{1}{J_1} - \frac{1}{J_2} \right) (\hat{L}_-^2 + \hat{L}_+^2), \quad (6a)$$

$$J_k = J_0 \sin^2(\gamma - k2\pi/3), \quad k = 1, 2, 3, \quad (6b)$$

and the eigenfunctions are

$$\psi_{I_n M} = \sum_K A_K^{I_n}(\gamma) |IMK\rangle, \quad (7a)$$

$$K = \begin{cases} 0, 2, 4, \dots, I & \text{for even } I, \\ 2, 4, 6, \dots, I-1 & \text{for odd } I, \end{cases} \quad (7b)$$

where  $|IMK\rangle$  are the wave functions of the axial rotor. The matrix elements of the Hamiltonian  $H$  are given in units of  $\hbar^2/J_0$  by

$$\begin{aligned} \langle IMK' | H | IMK \rangle &= \delta_{K'K} \left\{ \frac{1}{4} \left( \frac{J_0}{J_1} + \frac{J_0}{J_2} \right) [I(I+1) - K^2] + \frac{J_0}{2J_3} K^2 \right\} \\ &+ \delta_{K', K-2} \frac{J_0}{8} \left( \frac{1}{J_1} + \frac{1}{J_2} \right) [(I+K)(I-K+1)(I+K-1)(I-K+2)]^{1/2} \\ &+ \delta_{K', K+2} \frac{J_0}{8} \left( \frac{1}{J_1} + \frac{1}{J_2} \right) [(I-K)(I+K+1)(I-K-1)(I+K+2)]^{1/2}. \end{aligned} \quad (8)$$

After completing the establishment and diagonalization of the energy matrix for given angular momentum we obtain the energies  $\varepsilon_{I_n}$  and the wave functions  $\psi_{I_n M}$ , where  $n$  distinguishes among the different states with the

TABLE I. Energy spectra of triaxial rotor  $\varepsilon_I$  for  $\gamma = 10^\circ - 30^\circ$  in steps of  $5^\circ$ , in units of  $\hbar^2/J_0$ .

$I^\pi$	$\gamma$	$10^\circ$	$15^\circ$	$20^\circ$	$25^\circ$	$30^\circ$
g.s. band						
$2^+$		4.253	4.596	5.124	5.861	6.628
$4^+$		14.154	15.179	16.500	17.763	18.871
$6^+$		29.649	31.431	33.114	34.381	35.849
$8^+$		50.655	52.925	54.334	55.493	57.262
$10^+$		77.061	79.275	80.004	80.980	82.968
$12^+$		108.737	110.241	110.084	110.755	112.889
$\gamma$ band 1						
$2^+$		67.747	31.404	18.876	13.432	11.372
$3^+$		72.000	36.000	24.000	19.292	18.000
$4^+$		77.699	42.305	31.577	29.516	32.031
$5^+$		84.753	49.751	39.215	36.276	36.000
$6^+$		93.380	59.681	52.212	54.448	58.529
$7^+$		103.143	69.423	60.395	58.344	58.000
$8^+$		114.846	83.780	80.620	85.690	90.000
$9^+$		127.138	94.814	86.840	84.643	84.000
$10^+$		142.167	114.746	115.879	121.646	126.086
$11^+$		156.692	125.675	117.961	114.985	114.000
$12^+$		175.426	152.507	156.831	162.016	166.600
$\gamma$ band 2						
$4^+$		268.148	122.516	71.923	49.183	39.098
$5^+$		275.248	130.249	80.785	60.186	54.000
$6^+$		283.771	139.547	91.505	73.926	74.667
$7^+$		293.718	150.417	104.058	89.010	88.000
$8^+$		305.091	162.876	118.682	109.080	116.026
$9^+$		317.893	176.918	134.839	125.596	126.000
$10^+$		332.125	192.601	153.887	153.625	162.441
$11^+$		347.789	209.837	172.991	167.890	168.000
$12^+$		364.891	228.852	197.496	204.839	213.562

same  $I$ . Then the energy of the  $I_n$  level in the general asymmetric rotor model can be rewritten as

$$E_{I_n}(b) = a\varepsilon_{I_n}(1 - b\varepsilon_{I_n}), \quad (9)$$

where  $a \equiv \hbar^2/J_0$  and  $b$  can be used as free parameters. By the way, we point out that the energies of levels  $2_1^+$  and  $2_2^+$ ,  $\varepsilon_{2_1}$  and  $\varepsilon_{2_2}$ , obtained by diagonalizing the matrix Eq. (8) for  $I = 2$  are exactly equal to that given by Eq. (5) for any  $\gamma$ . In Table I the energy spectra of the triaxial rotor, in units of  $(\hbar^2/J_0)$ , obtained by the diagonalization method are listed for  $\gamma = 10^\circ - 30^\circ$  in steps of  $5^\circ$ .

With the energies listed in Table I we can easily get the staggering indices up to  $S(12)$  for different  $\gamma$ . The calculated  $S(I)$  for even  $I$  are given in Fig. 3. In order to see how the vibration-rotation interactions influence the behavior of the staggering indices, we have also calculated  $S(I_{\text{even}})$  for  $I = 4-12$  at different values of the parameter  $b$ . The results are shown in Fig. 4.

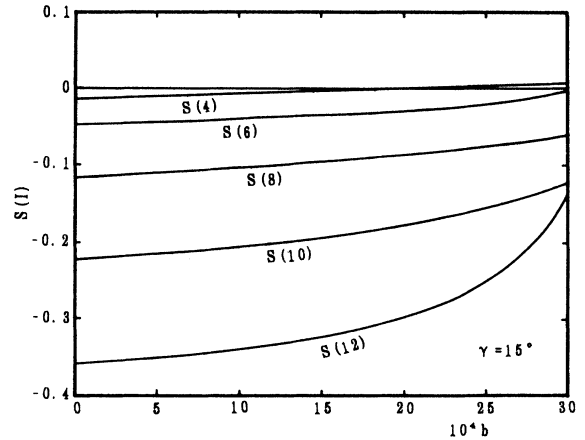


FIG. 4. Staggering indices  $S(I_{\text{even}})$  of a  $\gamma$ -rigid rotor for  $\gamma = 15^\circ$  as functions of the vibration-rotation coupling parameter  $b$ .

### III. DISCUSSION: IS THERE TRIAXIALITY IN LOW-SPIN LOW-ENERGY STATES OF NUCLEI?

It is evident from Fig. 2 that for a  $\gamma$ -soft rotor the indices  $S(I)$  for even  $I$  are positive at  $P = 0$  and decrease with increasing parameter  $P$ , and finally become negative with  $P$  greater than some fixed value depending on  $I$ . In contrast, the indices  $S(I_{\text{even}})$  for a  $\gamma$ -rigid rotor are always negative and the absolute values are increased with increasing  $\gamma$ . But when the vibration-rotation coupling is considered  $S(I)$  for even  $I$  may become positive if the parameter  $b$  is greater than certain values, while  $S(I)$  for odd  $I$  are still positive, as shown in Fig. 4. So we cannot undoubtedly distinguish a  $\gamma$ -soft and  $\gamma$ -rigid rotor according only to the value of  $S(4)$ . We need a group of  $S(I)$  or the zigzag plot of  $S(I)$  for this purpose. In fact, the zigzag patterns of  $S(I)$  for the  $O(6)+V_3$  model and the general triaxial rotor model are opposite in two respects (see Fig. 5): the former has positive zigzag phase and converges slowly as  $I$  increases for fixed parameter  $P$ ; while the latter has negative zigzag phase and diverges

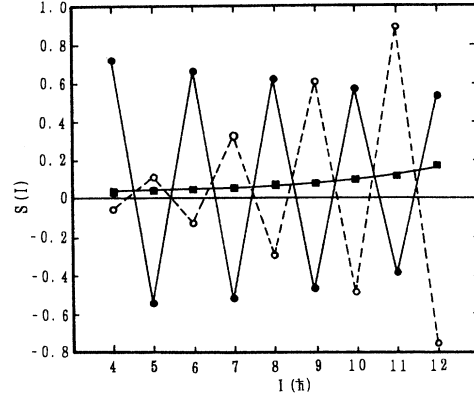


FIG. 5. Zigzag patterns of  $S(I)$  for broken  $O(6)$  symmetry with three-body potential and the general triaxial rotor model with vibration-rotation interactions. ■—■ Axial rotor,  $A = 60$ ,  $B = 0.15$ ; ●—● broken  $O(6)$  symmetry with  $V_3$ ,  $B = 62$ ,  $C = 12$ ,  $P = 1.5$ ; ○---○ triaxial rotor,  $\gamma = 20^\circ$ ,  $b = 0.003$ .

TABLE II. Candidates for triaxiality in low-energy low-spin states, and two examples of the axial rotor that are slightly  $\gamma$  soft, nuclei  $^{162}\text{Dy}$  and  $^{162}\text{Er}$ .

Nuclide	$R_4$	$\Delta$	$S(4)$ $S(5)$	$S(6)$ $S(7)$	$S(8)$ $S(9)$	$S(10)$ $S(11)$	Ref.
$^{78}\text{Ge}$	2.54	0.0893	-0.043				[12]
$^{78}\text{Kr}$	2.46	0.0237	0.256	0.078	-0.026	-0.124	[13]
$^{80}\text{Kr}$	2.33	0.0454	-0.045	0.031	0.131		[14]
$^{80}\text{Kr}$			0.296	0.143	0.068		
$^{98}\text{Ru}$	2.14	0.0261	-0.061	0.001			[14]
$^{98}\text{Ru}$			0.479	-0.308			[15]
$^{160}\text{Gd}$	3.30	0.0042	0.055				[16]
$^{160}\text{Gd}$			0.023	-0.012			
$^{164}\text{Dy}$	3.30	0.0085	-0.007				[16]
$^{164}\text{Dy}$			0.003	-0.002			
$^{170}\text{Er}$	3.31	0.0023	0.009				[16]
$^{170}\text{Er}$			0.040	-0.046			
$^{170}\text{Hf}$	3.19	0.0002	-0.059	0.165			[17]
$^{170}\text{Hf}$			-0.017				[17]
$^{180}\text{Hf}$	3.31	0.0067	-0.201				[16]
$^{180}\text{Hf}$			0.202				
$^{186}\text{W}$	3.24	-0.0019	-0.008				[16]
$^{186}\text{Pt}$	2.56	0.0340	-0.098				[18]
$^{192}\text{Os}$	2.82	0.0065	0.088	-0.062	-0.201		[19]
$^{192}\text{Os}$			0.071	0.193			
$^{192}\text{Pt}$	2.48	0.0086	0.167	-0.063	-0.241		[19]
$^{192}\text{Pt}$			0.099	0.282			
$^{194}\text{Pt}$	2.47	0.0294	0.116	-0.125	(-0.153) <sup>b</sup>		[20]
$^{194}\text{Pt}$			0.159	(0.243)			
$^{162}\text{Dy}^a$	3.29	0.0061	0.007	0.014	0.024	0.046	$S(12)$ 0.156
$^{162}\text{Dy}^a$			0.003	-0.002	-0.012	-0.039	-0.205
$^{162}\text{Er}^a$	3.23	0.0007	0.030	0.041	0.076	0.147	0.135
$^{162}\text{Er}^a$			-0.002	-0.016	-0.062	-0.132	

<sup>a</sup>Data are taken from Ref. [23].

<sup>b</sup>Numbers in parentheses are not undoubtedly determined.

rapidly as  $I$  increases for fixed parameter  $b$ . For comparison we also give the  $S(I)$ - $I$  plot for the axial rotor with vibration-rotation interactions (briefly described as the axial rotor model in the following), in which the energy spectra have the form

$$E_I = AI(I+1) - BI^2(I+1)^2. \quad (10)$$

It must be emphasized from Fig. 5 that for the axial rotor all the  $S(I)$  are positive and small in magnitude and show no zigzag behavior, but increase slowly with increasing  $I$ . Of course  $S(I) = 0$  for all  $I$  if  $B = 0$  in Eq. (10), as mentioned above. Evidently, zigzag plots are more effective signatures of  $\gamma$  softness or triaxiality than  $S(4)$  and/or  $S(6)$ . Thus when we have sufficient experimental data of  $\gamma$  bands from which the  $S(I)$ - $I$  plots can be obtained we may clearly distinguish  $\gamma$  soft, triaxial, and axial rotor.

Is there triaxiality in low-spin low-energy states of nuclei? A negative answer has been given by Zamfir and Casten as mentioned above [4]. But they have only considered  $S(4)$  and in some cases  $S(6)$ ; we want to work up to spin  $I = 12$  to see what will happen. For this purpose we have examined the experimental data of about 140 nuclides, for which the data of  $\gamma$  bands are available, in the mass region  $A = 64$ –200. We have found that (1) most of the nuclei with clear staggering in mass region  $A = 64$ –140 are  $\gamma$  unstable, at least  $\gamma$  soft; (2) almost all the axial nuclei in mass region  $A = 140$ –200 are slightly  $\gamma$  soft; (3) a few of the nuclei may be slightly triaxial in their ground states; and (4) some nuclei exhibit a kind of shape transition from  $\gamma$  soft to triaxial, even from axial to  $\gamma$ -soft to triaxial shape with increasing angular momentum  $I$ . In Table II all the candidates we found for the triaxial rotor in low-energy low-spin states are given, where  $R_4 = E_4/E_2$  and  $\Delta = (E_{2_1} + E_{2_2} - E_3)/(E_{2_1} + E_{2_2})$ . We should point out that  $\Delta = 0$  not only for the triaxial rotor but also for all ideal rotors with energy spectra

$E \propto I(I+1)$ . So the indices  $\Delta$  are given not as a signature of triaxiality but as a measure of the spectra deviating from the law  $I(I+1)$ .

Only five nuclei, that is,  $^{78}\text{Ge}$ ,  $^{170}\text{Hf}$ ,  $^{180}\text{Hf}$ ,  $^{186}\text{W}$ , and  $^{186}\text{Pt}$  (see Table II), have negative  $S(4)$ , and their absolute values are small except for  $^{180}\text{Hf}$  which has  $S(4) = -0.2$  and  $S(5) = +0.2$ ; they may be candidates for triaxiality in their ground states. Some discussion is appropriate of nuclei  $^{170}\text{Hf}$  and  $^{186}\text{Pt}$ . There are two  $2^+$  states that may be selected as  $2^+_\gamma$  in  $^{170}\text{Hf}$ : 961.3 and 987.0 keV levels. If we take the 961.3 keV level as the  $2^+_\gamma$  state and the 987 keV level as the  $2^+_\beta$  state, then  $\Delta = 0.024$  and  $S(4) = 0.081$ . If we take the 987 keV level as a  $2^+_\gamma$  state and the other as  $2^+_\beta$ , then  $\Delta = 0.00019$  and  $S(4) = -0.017$ . A similar situation appears in the nucleus  $^{186}\text{Pt}$ : when we take the 607.2 keV level as a  $2^+_\gamma$  state, then  $\Delta = -0.197$  and  $S(4) = 0.243$ . When we take the 798.5 keV level as a  $2^+_\gamma$  state then  $\Delta = 0.034$  and  $S(4) = -0.098$ . We prefer to select the one which gives the smaller  $\Delta$ , because all other nuclei have very small  $\Delta$ .

Most of the nuclei listed in Table II exhibit a kind of zigzag phase transition in the spin  $I = 5$ –7 region. This fact may be explained as a nuclear shape transition from  $\gamma$ -soft to triaxial shape. But the triaxial  $N = 76$  isotones  $^{132}\text{Ba}$ ,  $^{134}\text{Ce}$ ,  $^{136}\text{Nd}$ ,  $^{138}\text{Sm}$ , and  $^{140}\text{Gd}$  [21] have not been confined in the spin region  $I \leq 8$ . A very interesting example showing shape transition from axial to  $\gamma$ -soft to triaxial shape is provided by the nucleus  $^{164}\text{Er}$ . The  $S(I)$ - $I$  plot for the nucleus  $^{164}\text{Er}$  is given in Fig. 6 (experimental data are taken from Ref. [22]). It is evident that the  $S(I)$ - $I$  plot can be clearly divided into three sections:  $I \leq 8$  with  $S(I) > 0$ ,  $I = 9$ –14 with positive zigzag phase, and  $I = 15$ –19 with negative zigzag phase. The corresponding theoretical zigzag plots for axial,  $\gamma$ -soft, and triaxial rotor are also given in the same figure.

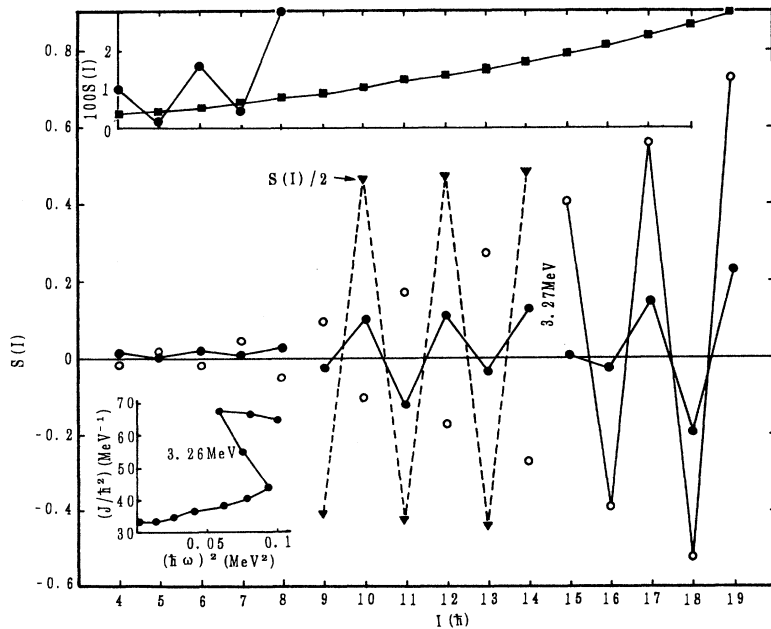


FIG. 6. Zigzag phase transitions in the  $S(I)$ - $I$  plot and the  $2J/\hbar^2 - (\hbar\omega)^2$  plot for nucleus  $^{164}\text{Er}$ . ●—● Experimental values [20,22]; ■—■ axial rotor; ▼—▼  $\gamma$ -soft rotor; ○—○ triaxial rotor.

The energy spectra from which the zigzag plots can be drawn for axial,  $\gamma$ -soft, and triaxial rotor are

$$E_I = 13.74I(I+1) - 0.0073[I(I+1)]^2,$$

$$E_I = 39.22\tau(\tau+3) + 1.60I(I+1) - 0.711\{[4\tau(\tau+3)]^2 + [I(I+1)]^2\}/(14)^2,$$

$$E_I = 20.74\varepsilon_I(1 - 0.00088\varepsilon_I), \quad \gamma = 12.52^\circ,$$

respectively. On the other hand, the  $\gamma$ -transition energies in the yrast band exhibit an anomalous decrease, which leads to a backbending  $J/\hbar^2 - (\hbar\omega)^2$  plot as shown in Fig. 6, at  $I = 16$  or excited energy  $E \sim 3400$  keV. This energy is just inside the region in which the zigzag phase for  $S(I)$  is of opposite sign from positive to negative. So we believe that there is indeed a kind of shape transition from axial passing through  $\gamma$ -soft to triaxial shape in nucleus  $^{164}\text{Er}$  with increasing  $I$ .

Two examples of axial nuclei that are slightly  $\gamma$  soft ( $^{162}\text{Dy}$  and  $^{162}\text{Er}$ ) are also listed in Table II. It is a general rule that the  $\gamma$  softness increases with increasing  $I$  for axial nuclei as shown by nuclei  $^{162}\text{Dy}$  and  $^{162}\text{Er}$ . This means that when the angular momentum  $I$  is greater than a certain value the axial shape will change to a  $\gamma$ -soft shape. How to explain this shape transition and that from  $\gamma$ -soft to triaxial shape using a microscopic theory is

a very interesting subject. We are quite sure that certain dynamic effects should be contained in such a theory.

#### IV. SUMMARY

We have studied the behaviors of the staggering indices  $S(I)$  in the axial and triaxial rotor model both with vibration-rotation interactions as well as in the broken  $O(6)$  symmetry of the IBM1 with a three-body potential. It has been found that the zigzag phases of  $\gamma$ -soft and  $\gamma$ -rigid rotors are exactly opposite, while no zigzag behavior appears in an  $S(I)$ - $I$  plot of the axial nucleus. Thus we use zigzag plots of  $S(I)$  to clearly distinguish  $\gamma$ -soft and triaxial shapes of nuclei. The zigzag plot is a more effective signature of  $\gamma$  softness or triaxiality than single  $S(4)$  or/and  $S(6)$ . With this signature we have examined the experimental data of about 140 nuclei in the mass region  $A = 64$ –200, and found that most of the nuclei are axial and slightly  $\gamma$  soft, or  $\gamma$  unstable, at least  $\gamma$  soft, but a few of them are triaxial in their ground or near ground states, while some of them exhibit a kind of shape transition from axial to  $\gamma$ -soft or/and  $\gamma$ -soft to triaxial shape. Lastly, we should emphasize that in order to distinguish undoubtedly  $\gamma$ -soft and triaxial shapes of nuclei more and more precise data of  $\gamma$  or quasi- $\gamma$  bands are needed.

- 
- [1] M. J. A. de Voigt, J. Dudek, and Z. Szymanski, *Rev. Mod. Phys.* **55**, 949 (1983); K. Hara and Y. Sun, *Nucl. Phys.* **A537**, 77 (1992).
- [2] R. F. Casten and P. Von Brentano, *Phys. Lett.* **152**, 22 (1985).
- [3] A. Leviatan, A. Novoselsky, and I. Talmi, *Phys. Lett.* **172**, 144 (1986).
- [4] N. V. Zamfir and R. F. Casten, *Phys. Lett. B* **260**, 265 (1991).
- [5] K. Heyde, P. Von Isacker, M. Waroquier, and J. Moreau, *Phys. Rev. C* **29**, 1420 (1984).
- [6] A. S. Davydov and G. F. Filippov, *Nucl. Phys.* **8**, 237 (1958).
- [7] Liao Ji-zhi and Wang Huang-sheng, *Phys. Rev. C* **49**, 2465 (1994).
- [8] C. A. Mallman, *Nucl. Phys.* **24**, 535 (1961).
- [9] R. F. Casten, N. V. Zamfir, P. Von Brentano, F. Seiffert, and W. Lieberz, *Phys. Lett. B* **265**, 9 (1991).
- [10] J. F. Suarez and E. Y. De Aisenberg, *Nucl. Phys.* **A90**, 449 (1967).
- [11] C. H. Townes and A. L. Schawlow, *Microwave Spectroscopy* (McGraw-Hill, New York, 1955).
- [12] W. T. Chou, D. S. Brenner, R. F. Casten, and R. L. Gill, *Phys. Rev. C* **47**, 157 (1993).
- [13] B. Singh, *Nucl. Data Sheets* **66**, 623 (1992).
- [14] B. Singh and D. A. Viggars, *Nucl. Data Sheets* **36**, 127 (1982).
- [15] G. S. Samudra, K. D. Cames, F. A. Rickey, P. C. Simms, and S. Zeghib, *Phys. Rev. C* **37**, 605 (1988).
- [16] P. C. Sood, D. M. Headly, and R. K. Sheline, *At. Data Nucl. Data Tables* **47**, 89 (1991).
- [17] Z. Chunmei, *Nucl. Data Sheets* **50**, 351 (1987).
- [18] R. B. Firestone, *Nucl. Data Sheets* **55**, 583 (1988).
- [19] V. S. Shirley, *Nucl. Data Sheets* **64**, 205 (1991).
- [20] S. A. Hjorth, A. Johnson, Th. Lindblad, L. Funke, P. Kemnitz, and G. Winter, *Nucl. Phys.* **A262**, 328 (1976); P. O. Hess, J. Maruhn, and W. Greiner, *J. Phys. G* **7**, 737 (1981).
- [21] E. S. Paul, K. Ahn, D. B. Fossan, Y. Liang, R. Ma, and N. Xu, *Phys. Rev. C* **39**, 153 (1989).
- [22] E. N. Shurshikov, *Nucl. Data Sheets* **47**, 433 (1986).
- [23] R. G. Helmer, *Nucl. Data Sheets* **64**, 79 (1991).